

## Initial state QED radiation at next-to-leading logarithmic accuracy for future $e^+e^-$ colliders

---

**Giovanni Stagnitto\***

*Physik-Institut, Universität Zürich,  
Winterthurerstrasse 190, CH-8057 Zürich, Switzerland*

*E-mail:* [giovanni.stagnitto@physik.uzh.ch](mailto:giovanni.stagnitto@physik.uzh.ch)

We present state-of-the-art results for the QED Parton Distribution Functions (PDFs), which have been recently pushed up to next-to-leading logarithmic (NLL) accuracy. NLL PDFs properly take into account the mixing between the electron/positron with the photon and the other fermions, running- $\alpha$  effects and the dependence on the renormalisation and factorisation scheme. We discuss the inclusion of NLL PDFs in the automated MADGRAPH5\_AMC@NLO framework, which have been equipped with next-to-leading order (NLO) electroweak corrections, and we present first NLL+NLO predictions for physical observables at lepton colliders.

*41st International Conference on High Energy physics - ICHEP2022  
6-13 July, 2022  
Bologna, Italy*

---

\*Speaker

It is not unreasonable to assume that the future of high-energy physics will involve an  $e^+e^-$  collider [1–4]. It is time for the theoretical community to start thinking about how to enlarge the legacy of LEP. The techniques and the calculations developed for LEP need to be revisited to keep up with the astonishing projected experimental error on measurements at future colliders. The relative error on several electroweak observables will reach 0.01% and possibly be even smaller [5].

The typical cross section relevant to  $e^+e^-$  collisions is in principle entirely computable as a perturbative series in the QED coupling constant  $\alpha$ . However, calculations of processes in QED always feature large contributions stemming from photon collinear emissions in the initial state (initial state radiation, ISR) [6]. These contributions appear as logarithms to some power of some hard physical scale  $Q$  over the mass of the electron  $m_e$ ,  $L = \log^k(Q^2/m_e^2)$ :

$$d\sigma_{e^+e^-} = \alpha^b \sum_{n=0}^{\infty} \alpha^n \left( c_0^{(n)} + c_1^{(n)} L + \dots + c_n^{(n)} L^n \right), \quad (1)$$

with  $b$  the power of  $\alpha$  in the Born process. These logarithmic terms can be numerically large, preventing the perturbative series from being well behaved.

It is fortunate that such  $\log^k(Q^2/m_e^2)$  terms are universal, hence they can be taken into account to all orders in  $\alpha$  by a process-independent resummation procedure. With the *collinear factorisation* approach, the physical cross section is written by means of a factorisation formula that recalls the standard QCD factorization formula at hadron colliders:

$$d\sigma_{e^+e^-} = \sum_{ij} \int dz_+ dz_- \Gamma_{i/e^+}(z_+, \mu^2, m_e^2) \Gamma_{j/e^-}(z_-, \mu^2, m_e^2) d\hat{\sigma}_{ij}(z_+, z_-, Q^2, \mu^2) + \mathcal{O}\left(\frac{m_e^2}{Q^2}\right). \quad (2)$$

Let us describe the various terms present in this equation:  $d\sigma_{e^+e^-}$  is the *particle-level* cross section, computed with massive electrons;  $d\hat{\sigma}_{ij}$  is a *parton-level* cross section, understood to be computed with massless electrons, which does not contain any logarithmic term, and is expected to be well-behaved order by order in perturbation theory;  $z_{\pm}$  are the longitudinal momentum fractions carried by the partons w.r.t. their mother particle;  $\Gamma_{i/e^{\pm}}$  are the Parton Distribution Functions (PDFs) of the electron or the positron, a name that originates from the analogy of Eq. (2) with its QCD counterpart. PDFs are universal and resum to all order the collinear logarithms due ISR. Note that the nature of the parton entering the short-distance cross section can coincide with that of the incoming particle e.g.  $(i, j) = (e^+, e^-)$ , or it can differ e.g.  $(i, j) = (\gamma, e^-), (e^-, e^-), \dots$ . Moreover, as in QCD, a suitable factorisation scheme must be introduced (e.g.  $\overline{\text{MS}}$ ) to regulate the zero-mass divergences in the parton-level cross section and a factorization scale  $\mu^2$  appears both in the  $\Gamma_{i/e^{\pm}}$  and in  $d\hat{\sigma}_{ij}$ .

At variance with hadronic PDFs, QED PDFs are entirely calculable with perturbative techniques. In the following, we will mostly focus on the PDFs relevant to an incoming unpolarised electron particle,  $\Gamma_{i/e^-} \equiv \Gamma_i$ ; the PDFs of an incoming positron are trivially related by charge conjugation. We will refer to  $\Gamma_{e^-}$  as electron PDF, and to  $\Gamma_{\gamma}$  as photon PDF. At the initial scale  $\mu_0^2 \simeq m_e^2$ , the leading order initial condition is a trivial  $\Gamma_{e^-}(z, \mu_0^2) = \delta(1-z)$ . The PDF at the final scale  $\mu^2$  can be obtained by means of QED DGLAP evolution equations [7–10]. At leading logarithmic (LL) accuracy i.e. the resummation of the dominant tower of  $(\alpha L)^k$  terms, analytical expressions have been known for a long time [8, 9, 11, 12]:

$$\Gamma_{e^-}^{\text{LL}}(z, \mu^2) = \frac{\exp[(3/4 - \gamma_E)\eta]}{\Gamma(1+\eta)} \eta (1-z)^{-1+\eta} - \frac{1}{2} \eta (1+z) + \mathcal{O}(\alpha^2), \quad \eta = \frac{\alpha}{\pi} L. \quad (3)$$

Such LL analytical expressions are built out of an additive matching between a recursive solution up to some order in  $\alpha$ , typically  $\mathcal{O}(\alpha^3)$ , and an all-order  $\alpha$  solution valid in the region  $z \rightarrow 1$ . Note that with  $Q$  of the order of a few hundred GeV's one obtains  $\eta \sim 0.05$ . Therefore, because of the  $(1-z)^{-1+\eta}$  factor, the PDF is very peaked towards  $z = 1$ , where it diverges with an integrable singularity. In general, such a peculiar structure of the PDFs requires a suitable re-parameterization of the phase-space [13] when numerically performing the convolution in Eq. (2).

In view of high-energy future colliders and the need for precise predictions, LL accuracy for QED PDFs is certainly insufficient. Moreover, theoretical systematics are not well defined in a LL-accurate picture. For instance, the value of  $\alpha$  in Eq. (3) is entirely arbitrary at LL: whether  $\alpha$  runs or not, or more generally in which renormalisation scheme  $\alpha$  is defined, are questions that arise only at higher orders. To improve on the LL result, one can calculate individual higher powers of  $\alpha^l L^k$  by means of fixed-order calculations (see e.g. [14] and references therein) or extend the resummed result to next-to-leading logarithmic (NLL) accuracy i.e. resumming also the tower of  $\alpha(\alpha L)^k$  terms. I will focus on the latter.

In Ref. [15], the electron, positron, and photon PDFs of the unpolarised electron have been calculated at NLL accuracy in the  $\overline{\text{MS}}$  factorisation and renormalisation scheme. The PDFs have been derived by solving the DGLAP equations both numerically and analytically, by using as initial conditions for the evolution the ones derived in Ref. [16]. In Ref. [17], these results have been improved in several directions: first, with a DGLAP evolution featuring multiple fermion families (leptons and quarks) in a variable flavour number scheme i.e. by properly including the respective mass thresholds; second, by taking into account an alternative factorisation scheme, the  $\Delta$  scheme [18], where the NLO initial condition are maximally simplified; third, by considering two alternative renormalisation schemes,  $\alpha(m_Z)$  and  $G_\mu$  schemes (where  $\alpha$  is fixed).

NLL PDFs ready for phenomenology can be obtained with the public code eMELA<sup>1</sup>. Such a code supersedes the one developed in Ref. [15] (ePDF), that was limited to the evolution with a single lepton in the  $\overline{\text{MS}}$  renormalisation and factorisation schemes. eMELA is a standalone code, and can be linked to any external program. Since a runtime evaluation of the numerical solution is likely too slow for phenomenological applications, the possibility is given to the user to output the PDFs as grids compliant with the LHAPDF [19] format, that can be employed at a later stage. Moreover, regardless of whether the numerical solution is computed at runtime or read from the grids, eMELA always switches to the analytical solution for  $z \rightarrow 1$ . eMELA can also provide one with PDFs with beamstrahlung effects, according to the procedure presented in Ref. [13].

In Ref. [17], eMELA has been linked to MADGRAPH5\_AMC@NLO [20, 21] in order to reach NLL accuracy for the PDFs and NLO accuracy (in the full electroweak theory) for the short-distance cross section, and obtain first NLL+NLO predictions for physical observables at lepton colliders. While MADGRAPH5\_AMC@NLO is widely used in the context of LHC simulations, it can also be employed for lepton collisions. Indeed, many results for leptonic collisions were already provided in Ref. [20], including NLO-QCD corrections but limited to the case of a strictly fixed centre-of-mass energy. The extension to the case with QED ISR and beamstrahlung has been documented in Ref. [13], whereas Ref. [17] describes the inclusion of NLO EW corrections to the short distance cross section, allowing for the computation of NLL+NLO observables after linking to eMELA.

<sup>1</sup>Available here: <https://github.com/gstagnit/eMELA>.

Here we focus on a single process,  $e^+e^- \rightarrow W^+W^-$ , at  $\sqrt{s} = 500$  GeV and we present results for the cumulative cross section defined as

$$\sigma(\tau_{\min}) = \int d\sigma \Theta\left(\tau_{\min} \leq \frac{M_{W^+W^-}^2}{s}\right), \quad (4)$$

with  $M_{W^+W^-}^2$  the invariant mass squared of the pair of final state vector bosons. The other  $2 \rightarrow 2$  processes considered in Ref. [17] (e.g.  $e^+e^- \rightarrow t\bar{t}$ ) behave in a similar way, and we find qualitatively similar results in the range  $\sqrt{s} \in [50, 500]$  GeV. Ratios of  $\sigma(\tau_{\min})$  for different settings of the PDFs are shown in Fig. 1 as a function of  $\tau_{\min}$ . The region close to  $\tau_{\min} = 1$  has to be taken with a grain of salt because it features unresummed purely soft logs.

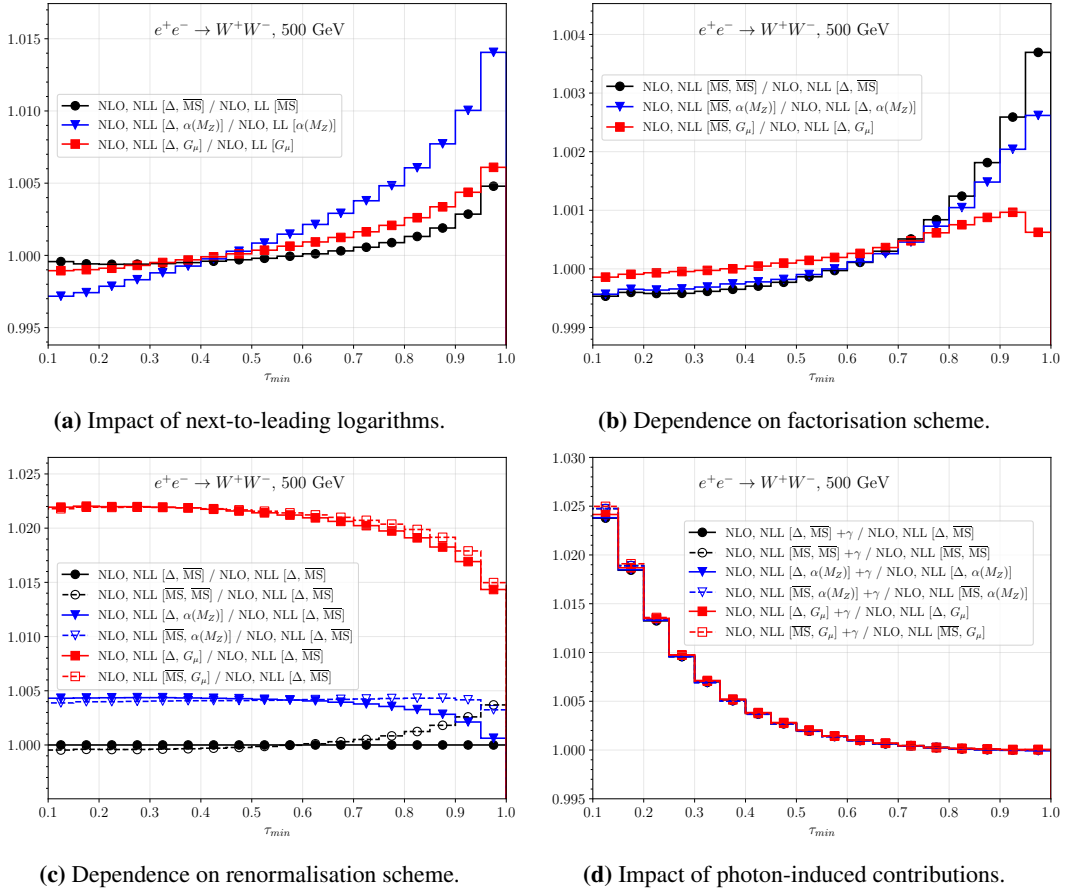


**Figure 1:** Cumulative cross section (4) for the  $e^+e^- \rightarrow W^+W^-$  process at  $\sqrt{s} = \mu = 500$  GeV. Several choices of accuracy (1a), factorisation (1b) and renormalisation (1c) schemes for the PDFs are shown. The notation adopted in the legends of the plots is: {accuracy of short-distance cross section}, {accuracy of PDF} [{factorisation scheme}, {renormalisation scheme}]. The accuracy of the short-distance cross section is always NLO in the full electroweak theory. The impact of the contribution coming from the  $\gamma\gamma$  channel (“+ $\gamma$ ”) is shown as well in (1d).

In Fig. 1a, the impact of NLL vs. LL PDFs is shown for three different choices of renormalisation schemes. It is clear that the corrections due to next-to-leading logarithms follow a

non-trivial pattern, impossible to account in some universal manner. Hence, NLL-accurate PDFs are phenomenologically important for precision studies.

In Fig. 1b, we show the dependence of the cumulative cross section on the adopted factorisation scheme. Such a dependence is of the order of  $10^{-4}$ - $10^{-3}$ , to be considered as a systematic error associated to the calculation. Note that the NLL electron PDF largely differs ( $\mathcal{O}(1)$ ) between the  $\overline{\text{MS}}$  and the  $\Delta$  scheme, with the NLL electron PDF in the  $\Delta$  scheme closer to the LL value [17]. Hence we can conclude that there are large cancellations between the PDFs and the short-distance cross section in the  $\overline{\text{MS}}$  scheme, cancellations which are absent for the  $\Delta$  scheme.

In Fig. 1c, we show the dependence of the cumulative cross section on the adopted renormalisation scheme. By comparing with Fig. 1b, we see that the renormalisation scheme dependence mostly leads to a normalisation effect, and it is significantly larger than the factorisation scheme one. The choice of the renormalisation scheme should be regarded as an informed choice rather than a systematic of the calculation.

Finally, in Fig. 1d, we consider the impact of photon-induced contributions for the process at hand. Such contributions are clearly visible in the region of small  $\tau_{\text{min}}$ , leading to a 1-2% difference between predictions. It is a physical effect independent on the choice of the renormalisation or factorisation scheme. The behaviour can be explained by a couple of considerations: at the Born level i.e.  $\mathcal{O}(\alpha^2)$ , the production of  $W^+W^-$  features a  $\gamma\gamma$  channel; the photon PDF  $\Gamma_\gamma$  is only suppressed by a power of  $\alpha$  w.r.t.  $\Gamma_{e^-}$ , with a peak at small- $z$  values. However, the magnitude of such an effect is process and observable dependent e.g. the impact of the  $\gamma\gamma$  channel for  $t\bar{t}$  production is practically negligible at the cumulative cross section level.

We refer the interested reader to Refs. [13, 15–18] for additional details about predictions at high-energy  $e^+e^-$  colliders within collinear factorisation and the usage of NLL PDFs. As a final remark, we would like to stress that moving towards NLL is important not only to improve on the accuracy of our predictions, but also needed for an assessment of sources of theoretical uncertainties.

The work presented in this contribution benefited from collaboration with V. Bertone, M. Cacciari, S. Frixione, M. Zaro and X. Zhao, to whom I am grateful. This work has received funding from the Swiss National Science Foundation (SNF) under contract 200020-204200.

## References

- [1] CEPC STUDY GROUP collaboration, *CEPC Conceptual Design Report: Volume 2 - Physics & Detector*, [1811.10545](#).
- [2] FCC collaboration, *FCC-ee: The Lepton Collider: Future Circular Collider Conceptual Design Report Volume 2*, *Eur. Phys. J. ST* **228** (2019) 261.
- [3] P. Bambade et al., *The International Linear Collider: A Global Project*, [1903.01629](#).
- [4] CLICDP, CLIC collaboration, *The Compact Linear Collider (CLIC) - 2018 Summary Report*, [1812.06018](#).
- [5] LCC PHYSICS WORKING GROUP collaboration, *Tests of the Standard Model at the International Linear Collider*, [1908.11299](#).

- [6] S. Frixione et al., *Initial state QED radiation aspects for future  $e^+e^-$  colliders*, in *2022 Snowmass Summer Study*, 3, 2022 [2203.12557].
- [7] G. Altarelli and G. Parisi, *Asymptotic Freedom in Parton Language*, *Nucl. Phys. B* **126** (1977) 298.
- [8] V.N. Gribov and L.N. Lipatov, *Deep inelastic  $e p$  scattering in perturbation theory*, *Sov. J. Nucl. Phys.* **15** (1972) 438.
- [9] L.N. Lipatov, *The parton model and perturbation theory*, *Yad. Fiz.* **20** (1974) 181.
- [10] Y.L. Dokshitzer, *Calculation of the Structure Functions for Deep Inelastic Scattering and  $e^+e^-$  Annihilation by Perturbation Theory in Quantum Chromodynamics.*, *Sov. Phys. JETP* **46** (1977) 641.
- [11] M. Skrzypek and S. Jadach, *Exact and approximate solutions for the electron nonsinglet structure function in QED*, *Z. Phys. C* **49** (1991) 577.
- [12] M. Cacciari, A. Deandrea, G. Montagna and O. Nicosini, *QED structure functions: A Systematic approach*, *Europhys. Lett.* **17** (1992) 123.
- [13] S. Frixione, O. Mattelaer, M. Zaro and X. Zhao, *Lepton collisions in MadGraph5\_aMC@NLO*, **2108.10261**.
- [14] J. Blümlein and K. Schönwald, *High-precision QED initial state corrections for  $e^+e^- \rightarrow \gamma^*/Z^*$  annihilation*, *Mod. Phys. Lett. A* **37** (2022) 2230004 [2202.08476].
- [15] V. Bertone, M. Cacciari, S. Frixione and G. Stagnitto, *The partonic structure of the electron at the next-to-leading logarithmic accuracy in QED*, *JHEP* **03** (2020) 135 [1911.12040].
- [16] S. Frixione, *Initial conditions for electron and photon structure and fragmentation functions*, *JHEP* **11** (2019) 158 [1909.03886].
- [17] V. Bertone, M. Cacciari, S. Frixione, G. Stagnitto, M. Zaro and X. Zhao, *Improving methods and predictions at high-energy  $e^+e^-$  colliders within collinear factorisation*, *JHEP* **10** (2022) 089 [2207.03265].
- [18] S. Frixione, *On factorisation schemes for the electron parton distribution functions in QED*, *JHEP* **07** (2021) 180 [2105.06688].
- [19] A. Buckley, J. Ferrando, S. Lloyd, K. Nordström, B. Page, M. Rüfenacht et al., *LHAPDF6: parton density access in the LHC precision era*, *Eur. Phys. J. C* **75** (2015) 132 [1412.7420].
- [20] J. Alwall, R. Frederix, S. Frixione, V. Hirschi, F. Maltoni, O. Mattelaer et al., *The automated computation of tree-level and next-to-leading order differential cross sections, and their matching to parton shower simulations*, *JHEP* **07** (2014) 079 [1405.0301].
- [21] R. Frederix, S. Frixione, V. Hirschi, D. Pagani, H.S. Shao and M. Zaro, *The automation of next-to-leading order electroweak calculations*, *JHEP* **07** (2018) 185 [1804.10017].